PROC. OF JSCE,
NO. 219, NOV. 1973

SECONDARY FLOW IN A BEND OF TURBULENT STREAM

By Hideo KIKKAWA, Syunsuke IKEDA**, Hideo OHKAWA*** and Yukio KAWAMURA****

SYNOPSIS

The flow at a bend of finite width, which is in equilibrium, is treated. The velocity distribution of the secondary flow is obtaind theoretically at the cross section of a channel by taking account of the thickness of the turbulent boundary layer which develops from the outer wall of a channel. The experimental investigations are also made, and compared with the theoretical works, which shows that the calculations agree well with the experiments.

1. INTRODUCTION

Under natural conditions, the streams become rarely rectilinear, but usually take winding courses called "meandering". The bend of the stream is also seen at the confluence of the rivers and at the division of the flow into two streams. Therefore, in studying the river mechanics, the knowledge of the flow at bend is quite necessary in connection with the problems such as deposition and scouring in bend, the dispersion of material in rivers, selective withdrawal from two-layer stratified flow in bend, etc.

One of the characteristics of the flow at bends is the superelevation of the free surface due to the presence of the centrifugal force. The second is the circulatory motion which flows toward the inside at the lower layer, and toward the outside at the upper layer. The cause of this circulatory motion is the difference in the centrifugal forces between the two layers. The existence of the secondary flow changes the structures of the flow, and consequently the shear distribution at bend. The circulatory flow intensifies the momentum exchange between the upper and the lower layer, which results in the redistribution of the velocity of the main flow in the vertical and radial directions. When the materials such as salt, silt, etc., are contained in the stream, the existence of the secondary flow increases the mixture between the two layers.

In 1876 J. Thompson found the existence of the secondary flow experimentally at the bend of a channel. Later on many researchers treated this problem. Böss (1934) evaluated the transverse superelevation by assuming the free-vortex velocity distribution of the main flow in the radial direction, and compared the results with experiments. Mockmore (1944) showed theoretically that the streamline at bend is hericoidal. Shukry (1950) investigated this problem experimentally. His experiments show the effect of the Reynolds number, the depth-width ratio, the radius-width ratio, and the deflection angle of bend. Einstein and Harder (1954) analysed the effect of the secondary flow back onto the cross distribution of the main flow. The Russian investigator, Rozovskii (1957) studied the distribution of the secondary flow, the radial distribution of the main flow, and the development of the secondary flow at the entrance region of a bend. Moreover, he tried to calculate the modified velocity distribution of the main flow in the vertical direction due to the secondary flow. Yen (1965) presented the results of experiments, which cover the velocity and the boundary-shear distributions, the transverse superelevation, and the development and the decay of the spiral mation. He also derived the distribution of the secondary flow by assuming that the flow is subcritical and the width-depth ratio of the channel is sufficiently large. Muramoto (1966) investigated the transverse superelevation and the distribution of the secondary flow at the entrance region in detail.

However, the effect of side wall has seldom

* Dr. Eng., Professor, Dept. of Civil Eng., Tokyo Institute of Technology.
** Research Associate, Dept. of Civil Eng., Tokyo Institute of Technology.
*** Research Associate, Dept. of Civil Eng., Niigata University.
**** Graduate Student, Dept. of Civil Eng., Tokyo Institute of Technology.

been taken into account in the papers mentioned above, and the velocity distribution of the secondary flow were calculated by assuming that the width of a stream is very large. Moreover, the velocity of the secondary flow becomes infinite at the bottom, because the above mentioned authors used the logarithmic velocity distribution for the main flow along the vertical.

Therefore, the main purposes of this paper are as follows:

(1) how does the width of a stream affect the velocity distribution of the secondary flow.

(2) how should the "virtual bottom" be determined so as not to make the velocity of the secondary flow infinite at the bottom.

In analysing these problems, it is assumed that the length of bend is sufficiently large, and the flow pattern does not change in the longitudinal direction. According to Goncharov and our experiment (5), the velocity distribution was established and the stream gained stable state when the stream flowed down more than 130° around the bend from the entrance. Therefore, the derivatives of the hydraulic variables with respect to Θ are equal to zero.

The method developed in this paper is applicable to the actual rivers, and the magnitude of the secondary flow can be estimated.

2. GOVERNING EQUATIONS OF THE SECONDARY FLOW

It is assumed that the flow is in equilibrium, and the eddy viscosity ε is constant within the cross section of a rectangular channel. If the channel has a complicated cross section, the eddy viscosity will change in the radial direction and the assumption made here will not be appropriate. However, as the informations of the eddy viscosity in the actual rivers are quite limited, we assumed the eddy viscosity is constant in the cross section of a rectangular channel not to make the calculation complicated. Following these assumptions, the equations of motion which are written in the cylindrical coordinates are:

$$U\frac{\partial U}{\partial R}+W\frac{\partial U}{\partial Z}-\frac{V^2}{R}=-\frac{1}{\rho}\frac{\partial P}{\partial R}+\varepsilon\left(\nabla^2 U-\frac{U}{R^2}\right) \quad \cdots\cdots(1)$$

$$U\frac{\partial W}{\partial R}+W\frac{\partial W}{\partial Z}=-g\cos i-\frac{1}{\rho}\frac{\partial P}{\partial Z}+\varepsilon\nabla^2 W \quad \cdots\cdots(2)$$

where

$$\nabla^2=\frac{\partial^2}{\partial R^2}+\frac{1}{R}\frac{\partial}{\partial R}+\frac{\partial^2}{\partial Z^2}$$

i=inclination of the free surface in the longitudinal direction, and U, V, W=velocity components of the radial, longitudinal, and vertical directions, respectively. The pressure terms can be eliminated from the above two equations by cross differentiation, and one obtains the equation written in the vorticity form,

$$U\frac{\partial \xi}{\partial R}+W\frac{\partial \xi}{\partial Z}-\frac{U}{R}\xi=\frac{2V}{R}\frac{\partial V}{\partial Z}+\varepsilon\left(\nabla^2-\frac{1}{R^2}\right)\xi \quad \cdots\cdots(3)$$

where

$$\xi=\frac{\partial U}{\partial Z}-\frac{\partial W}{\partial R}$$

From the continuity equation,

$$\frac{\partial}{\partial R}(RU)+\frac{\partial}{\partial Z}(RW)=0 \quad \cdots\cdots(4)$$

we can define the stream function of the secondary flow,

$$U=\frac{1}{R}\frac{\partial \psi}{\partial Z}, \qquad W=-\frac{1}{R}\frac{\partial \psi}{\partial R} \quad \cdots\cdots(5)$$

Substituting U and W in equation (3), we obtain after multiplying the both sides of the equation by R,

$$\frac{\partial \psi}{\partial Z}\frac{\partial \xi}{\partial R}-\frac{\partial \psi}{\partial R}\frac{\partial \xi}{\partial Z}-\frac{\xi}{R}\frac{\partial \psi}{\partial Z}=2V\frac{\partial V}{\partial Z}+\varepsilon\left(\frac{\partial^4\psi}{\partial R^4}+2\frac{\partial^4\psi}{\partial R^2\partial Z^2}+\frac{\partial^4\psi}{\partial Z^4}-\frac{2}{R}\frac{\partial^3\psi}{\partial R\partial Z^2}-\frac{2}{R}\frac{\partial^3\psi}{\partial R^3}+\frac{2}{R^2}\frac{\partial^2\psi}{\partial R^2}-\frac{3}{R^3}\frac{\partial \psi}{\partial R}\right) \quad \cdots\cdots(6)$$

If it is assumed, furthermore, that the channel has a sufficiently large radius and the nonlinear terms in the right hand side are small, the terms containing $1/R$ and the nonlinear terms can be ignored. The magnitude of the terms neglected will be evaluated later, and will be compared with the other terms. Then, the equation becomes finally

$$\frac{\partial^4\psi}{\partial R^4}+2\frac{\partial^4\psi}{\partial R^2\partial Z^2}+\frac{\partial^4\psi}{\partial Z^4}=-\frac{2}{\varepsilon}V\frac{\partial V}{\partial Z} \quad \cdots\cdots(7)$$

This is the fundamental equation which governs the motion of the secondary flow.

3. VIRTUAL BOTTOM AND BOUNDARY CONDITIONS

If logarithmic velocity distribution, $V/V_*=A+5.75\log(Z/K_s)$, is used for the distribution of the main flow, the term containing $V\partial V/\partial V$ in

equation (7) becomes infinite at the bottom, $Z=0$, and consequently the velocity of the secondary flow becomes infinite at the bottom. This does not indicate actual phenomenon. To avoid this situation, the authors introduce the virtual bottom defined as the thickness of the boundary layer which develops from the outer wall of a channel due to the existence of the bed. The scheme is is shown in Fig. 1.

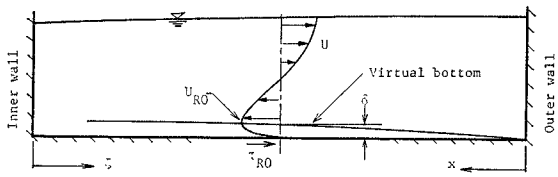

Fig. 1 Scheme of the Secondary Flow at Bend.

At the height δ, the gradient of U is equal to zero, and consequently the shear stress τ_R also extinguishes. The forces are, therefore, in equilibrium in the boundary layer. Then, the velocity distribution of the secondary flow can be calculated in the region except the thin layer δ, and it can be avoided that the velocity of the secondary flow becomes infinite at the bottom. In the following, the method of evaluation of the boundary layer thickness will be presented. The condition of equilibrium in the thickness of the boundary layer is

$$\rho\int_0^\delta \frac{V^2}{R}dRdZ+\tau_{R0}dR=\rho g i_R\delta dR \quad \cdots\cdots(8)$$

, in which the term containing V^2/R can be neglected, because V is very small in the thin layer δ. Then, equation (8) reduces to

$$\tau_{R0}=\rho g i_R\delta \quad \cdots\cdots(9)$$

The development of the boundary layer thickness and the shear stress at the bottom are expressed as follows:

$$\frac{\delta}{x}=0.38\left(\frac{\nu}{U_{R0}x}\right)^{\frac{1}{5}} \quad \cdots\cdots(10)$$

$$\frac{\tau_{R0}}{\rho U_{R0}^2}=0.029\left(\frac{\nu}{U_{R0}x}\right)^{\frac{1}{5}} \quad \cdots\cdots(11)$$

where x=distance from the outer wall. If they are evaluated at the center of a channel, the values of δ and τ_{R0} become

$$\frac{\delta}{B}=0.19\left(\frac{2\nu}{U_{R0}B}\right)^{\frac{1}{5}} \quad \cdots\cdots(12)$$

$$\frac{\tau_{R0}}{\rho U_{R0}^2}=0.029\left(\frac{2\nu}{U_{R0}B}\right)^{\frac{1}{5}} \quad \cdots\cdots(13)$$

Concerning the inclination of the free surface in the radial direction, it is derived by Ippen and Drinker for the forced-vortex velocity distribution of the flow in the transverse direction. It is written by

$$i_R=\frac{V_a^2}{gR_c}\frac{1}{1+\dfrac{B^2}{12R_c^2}} \quad \cdots\cdots(14)$$

Substituting (13), (12), and (14) in (9), the velocity of the secondary flow at the bottom is given by

$$U_{R0}=\left(6.43\frac{B}{R_c}\frac{1}{1+\dfrac{B^2}{12R_c^2}}\right)^{\frac{1}{2}}V_a \quad \cdots\cdots(15)$$

From equation (12), the thickness of the boundary layer is calculated. The plane displaced above the bottom by δ is supposed as the "virtual bottom." By introducing this bottom, the value of $V\dfrac{\partial V}{\partial Z}$ becomes finite even if the logarithmic law is employed for the velocity distribution of the longitudinal component along the vertical.

In our experiments, the width-depth ratio B/R_c was 1/4.5, and consequently the velocity of the secondary flow at the bottom U_{R0} is estimated greater than V_a, that is, $U_{R0}=1.2V_a$ in the equation (15). This is because the term $\rho\int_0^\delta \frac{V^2}{R}dRdZ$ in equation (8) was neglected and the Reynolds stress at the height δ was set equal to zero. Then, it gives rise to a fear that the height δ is estimated too small, and consequently the magnitude of the secondary flow is estimated too large. If U_{R0} is chosen as $0.12V_a$ (this value is physically reasonable when compared with the experiment), the value of δ becomes 1.58 times that of the case of $1.2V_a$ in the equation (12). Then, the velocity distribution of the secondary flow can be obtained from (22), (23) and (24). The result of calculation (Run R1) shows that the magnitude of the secondary flow at the bottom for the case of $0.12V_a$ is 0.78 times the case of $1.2V_a$. The value agrees well with the experimental result better than the case of $1.2V_a$ in the lower region of the cross section. The convergence of calculation is quite rapid and the first approximate value of the secondary flow at the bottom estimated by (15) can be safely used in the engineering sense.

The boundary conditions for ψ is expressed as

$$\begin{array}{ll} R=R_i & \psi=0 \\ R=R_o & \psi=0 \\ Z=0 \text{ (virtual bottom)} & \psi=0 \\ Z=H & \psi=0 \end{array} \quad \cdots\cdots(16)$$

which implies that the value of stream function is zero at the boundary, because there can be no

flux through the boundary. The nonslip condition at the side walls and the bottom are not imposed here.

4. VELOCITY DISTRIBUTION OF THE MAIN FLOW IN THE CROSS SECTION OF A CHANNEL

When the width-depth ratio is large, say, more than 10, the effect of side walls is relatively small, and the velocity of the flow may be described by the logarithmic distribution even in the curvilinear channel. As a consequence of the displacement of the bottom, the velocity of the main flow in the cross section of a channel which has rough bottom is given by

$$\frac{V}{V_0}=f\left(\frac{R}{R_c}\right)\frac{\log\frac{Z+\delta}{K_s}}{\log\frac{H+\delta}{K_s}} \quad \cdots\cdots(17)$$

where V_0=velocity of the free surface at the center of a channel, $f(R/R_c)=R/R_c$, and K_s=roughness of the bottom. The forced-vortex distribution is adopted for the velocity of the main flow, because this type of flow is most frequently seen at the fully developed region. If equation (17) is averaged over a cross section, V becomes

$$\frac{V}{V_a}=\frac{R}{R_c}\frac{\log\frac{Z+\delta}{K_s}}{\log\frac{H+\delta}{K_s}+\frac{\delta}{H}\log\left(\frac{H}{\delta}+1\right)-1} \quad \cdots\cdots(18)$$

Then, $V\partial V/\delta Z$ in equation (7) is expressed by

$$V\frac{\partial V}{\partial Z}=\frac{R^2}{R_c^2}V_a^2\times\frac{\log\frac{Z+\delta}{K_s}}{(Z+\delta)\left\{\log\frac{H+\delta}{K_s}+\frac{\delta}{H}\log\left(\frac{H}{\delta}+1\right)-1\right\}^2} \quad \cdots\cdots(19)$$

When the width-depth ratio is relatively small, smaller than 10, the logarithmic law is not applicable any more by the influence of the side walls. In this case, the velocity distribution of quadratic parabola which is proposed by Boussinesq is appropriate. It is expressed by

$$\frac{V}{V_a}=\frac{R}{R_c}\frac{1-K\left(1-\frac{Z}{H}\right)^2}{1-\frac{K}{3}} \quad \cdots\cdots(20)$$

where K=parameter determined by the ratio V_a/V_0, and is equal to $3(1-V_a/V_0)$. The term, $V\partial V/\partial V$, is given by

$$V\frac{\partial V}{\partial Z}=\frac{R^2}{R_c^2}\frac{V_a^2}{H}\left(1-\frac{Z}{H}\right)\frac{2K\left\{1-K\left(1-\frac{Z}{H}\right)^2\right\}}{\left(1-\frac{K}{3}\right)^2} \quad \cdots\cdots(21)$$

5. VELOCITY DISTRIBUTION OF THE SECONDARY FLOW

In order to get the velocity distribution of the secondary flow, equation (7) must be solved under the boundary condition (16). The stream function ϕ is expanded by the Fourier series,

$$\phi=\sum_{l,m=1}^{\infty}A_{lm}\sin\frac{l\pi Z}{H}\sin\frac{m\pi\zeta}{B} \quad \cdots\cdots(22)$$

where ζ is a new coordinate introduced in the radial direction for convenience, and is equal to the distance from the inner wall (Fig. 1). Substituting (22) in (7), one obtains after some arrangements,

$$A_{lm}=-\frac{8}{\varepsilon}\frac{1}{HB\pi^4}\times\frac{\int_0^B\int_0^H V\frac{\partial V}{\partial Z}\sin\frac{l\pi Z}{H}\sin\frac{m\pi\zeta}{B}dZd\zeta}{\left\{\left(\frac{l}{H}\right)^2+\left(\frac{m}{B}\right)^2\right\}^2} \quad \cdots\cdots(23)$$

, in which $V\partial V/\partial Z$ is given by (19) or (21) according to the magnitude of the width-depth ratio. Then, the velocity components of the secondary flow, U and W, can be calculated by

$$U=\frac{1}{R_i+\zeta}\frac{\partial\phi}{\partial Z}, \quad W=-\frac{1}{R_i+\zeta}\frac{\partial\phi}{\partial R} \quad \cdots(24)$$

6. EXPERIMENTAL APPARATUS, PROCEDURES AND DATA

A curving channel with dimensions, B=100 cm, R_c=450 cm, and Θ_c=306°, was prepared for the experiments. The slope of the bottom in the longitudinal direction is 1/500, which is fixed and can not be changed. The channel had a head and a tail tank. They were connected by a pump to recirculate water (Q_{max}=187 lit/sec). A sharp-crested weir of rectangular type were installed at the outlet of the head tank to measure the discharge. A straight reach of 2 m is prepared ahead the bend to adjust the flow condition. In the straight reach, concrete cylinders were placed and screens were inserted just downstream the cylinders. An adjustable tail gate was built at the end of the channel to control the depth of the flow. The layout of the channel is shown in Fig. 2. A standard Pitot tube was used to

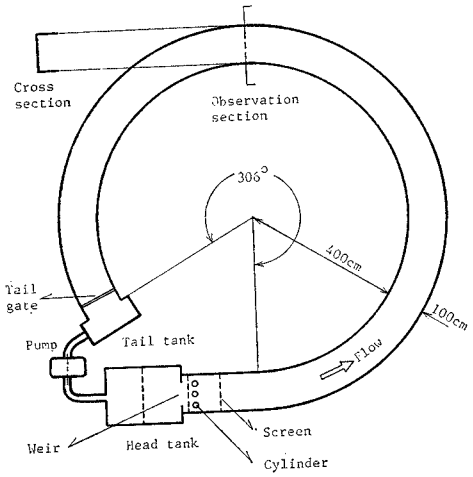

Fig. 2 Layout of the Circular Channel.

measure the velocity and piezometric head. The direction of the flow was measured by a light thread made of silk which was attached to the Pitot tube. Thus, we can divide the velocity into the tangential and the radial components. However, the vertical component could not be obtained, because it was too small to be measured except the region close to the wall. Since the roughness of the bottom was supposed as one of the factors which influence the secondary flow, the experiments were conducted for the rough bottom. The rough bottom was constructed by attaching sands, which have mean diameter $d_{50}=0.18$ cm, to the bottom of the circular channel. Another important factor which affects the flow pattern is the width-depth ratio. To investigate this effect, the depth of the flow was changed, and the following data were obtained.

Run bottom	Q (l/s)	H (cm)	V_a (cm/s)	B/H	Fr	Re ($\times 10^4$)	i ($\times 10^{-4}$)
R1 rough	30	7.0	42.9	14.3	0.52	2.63	5.7
R2 rough	80	20.0	40.0	5.0	0.29	5.72	5.7

The velocity distribution of the longitudinal and the radial components are shown in Figs. 3, 4, 5, and 6.

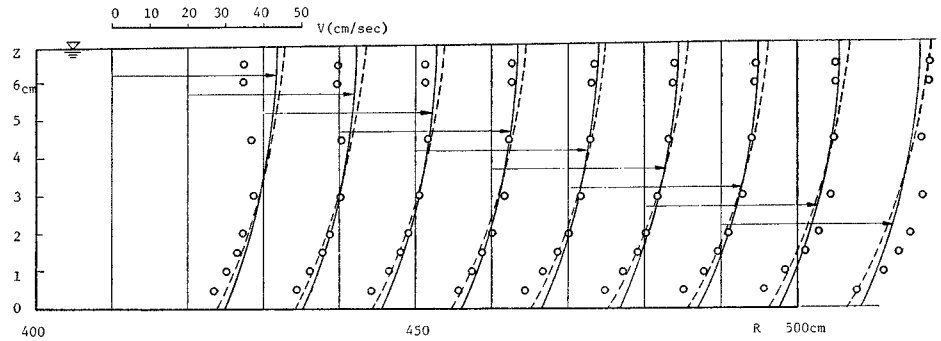

Fig. 3 Comparison of Longitudinal Velocity Computed from (18) and (20) with Experiment
Solid Line: Distribution of Quadratic Parabola ($K=0.3$)
Broken Line: Logarithmic Distribution ($\delta=1.71$ cm) Run R1

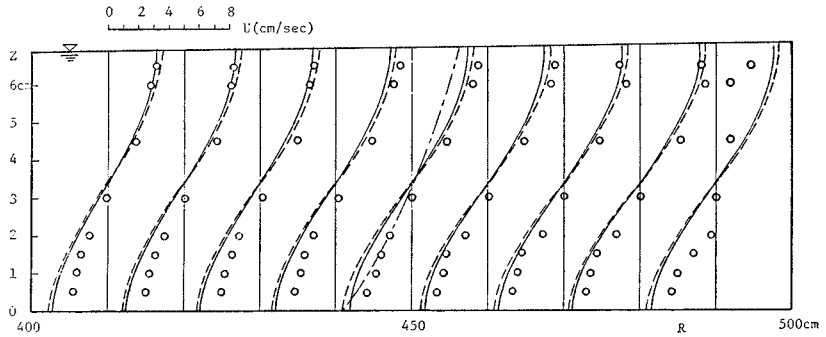

Fig. 4 Comparison of Radial Velocity Computed from (24) with Experiment.
Solid Line: Computed from Quadratic Parabola ($K=0.3$)
Broken Line: Computed from logarithmic law ($\delta=1.71$ cm) Run R1
Dot-dash-line: Rezovskii's Formula

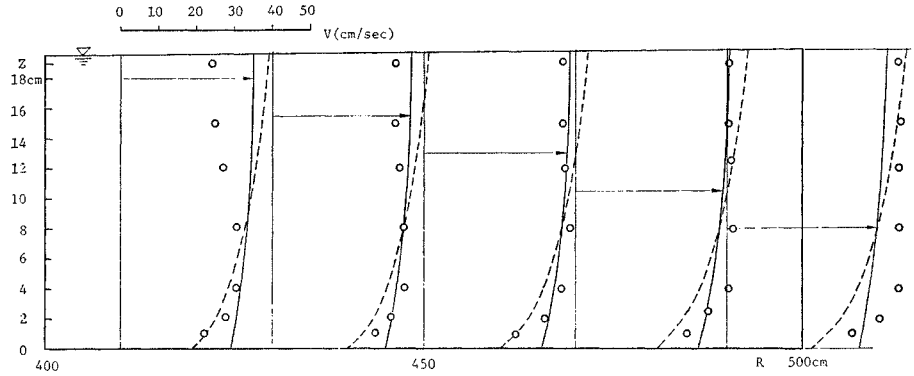

Fig. 5 Comparison of Longitudinal Velocity Computed from (18) and (20) with experiment.
Solid Line: Distribution of Quadratic Parabola ($K=0.167$)
Broken Line: Logarithmic Distribution ($\delta=1.73$ cm) Run R2

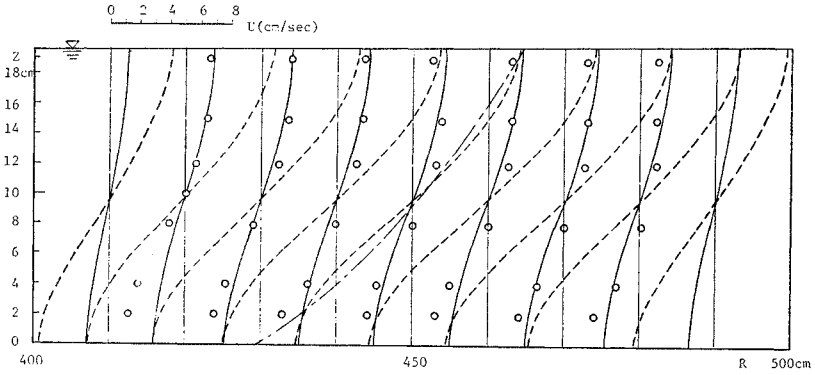

Fig. 6 Comparison of Radial Velocity Computed from (24) with Experiment.
Solid Line: Computed from Quadratic Parabola ($K=0.167$)
Broken Line: Computed from Logarithmic Law ($\delta=1.73$ cm) Run R2
Dot-dash-line: Rozovskii's Formula

7. DISCUSSIONS

Calculations of the secondary flow by equation (7) were performed for Run R1 and R2. For the case of Run R1, which had a large width-depth ratio of 14.3, the logarithmic distribution of the main flow is applicable as mentioned in Chapter 2. In Fig. 3, the distribution of the quadratic parabola and the logarithmic distribution are both plotted, in which the parameter involved in equation (20) is chosen as 0.3, and the displacement of the virtual bottom is calculated as 1.71 cm from equation (12). The shapes of the distributions differ very little each other. Therefore, the logarithmic law gives a good approximation of the distribution of the main flow in the vertical direction. Concerning the lateral distribution of the main flow, the forced-vortex distribution is appropriate as will be found in Fig. 3 and Fig. 5. The result of calculation for the secondary flow is compared with the experiment in Fig. 4, which shows good agreement. With respect to R2, which had a relatively small width-depth ratio of 5.0, the logarithmic law is not applicable any more, and the distribution of the quadratic parabola must be used. In Fig. 6, however, the results of calculation by using the logarithmic law and the quadratic parabola are both plotted to examine the agreement with the experiment. In the calculation, the parameter K involved in the quadratic parabola (20) is chosen as 0.167. It is easily seen from Fig. 6 that the logarithmic distribution (18) gives a larger value than experiment. The reason for it is that the logarithmic law has a larger gradient in the vertical than real, which is shown in Fig. 5. For comparison, the formula derived by Rozovskii,

$$\frac{U}{V_a}=\frac{1}{\kappa^2}\frac{H}{R_c}\left\{F_1(\eta)-\frac{\sqrt{g}}{\kappa C}F_2(\eta)\right\}$$

is plotted in Fig. 4 and Fig. 6. Rozovskii's formula, however, is only applicable to the central portion of a bend. His formula was obtained by assuming the logarithmic distribution for the main flow, and the effect of side wall was not taken into account. Therefore, it estimates the magnitude of the secondary flow larger than the actual in the case of small width-depth ratio as Run R2.

The neglected terms in (6), the nonlinear terms and the terms divided by R, were estimated after the calculation of U and W. It was found that their magnitudes were at most 10% at the close region to the wall where the values became the largest. Except in this region, their magnitudes were very small. The effect of side wall was limited in the region near the wall.

Recapitulating, the method of the calculation of secondary flow will be written in the follows:

(1) At first, estimate the transverse slope by using (14).

(2) The situation of the virtual bottom can be determined from (15) and (12).

(3) The stream function of the secondary flow is obtained by using (23) and (22). The term $V\partial V/\partial Z$ involved in (23) is determined by (19) or (21) according to the width-depth ratio. Eddy viscosity ε in (23) is equal to $V_*H/15$.

(4) Then, the velocity of the secondary flow in the cross section of a channel is determined by (24).

The method developed here is applicable to the actual rivers, and the magnitude of the secondary flow can be estimated. The knowledge of the secondary flow in bend is quite important as mentioned in the introduction. Especially in the problems mentioned previously, the effect of secondary flow on the dispersion of soluble matter will be discussed in another paper.

The authors solved the full Navier-Stokes equations of motion for laminar stream at bend by using the relaxation method in another paper (4). In the paper, the effects of nonlinear terms and the terms divided by R, which can not be neglected when the width-depth ratio is small, were discussed.

8. CONCLUSIONS

Through the investigation mentioned above, the following conclusions are obtained.

When the width-depth ratio is smaller than 10, the logarithmic distribution of the main flow in the vertical can not be used in calculating the secondary flow. In such a case, the distribution of the quadratic parabola gives a good result.

For natural rivers, which have usually very large width-depth ratio, the logarithmic law can be applied in the estimation of the secondary flow by considering the virtual bottom.

The effect of side wall is limited within the close region to the wall.

For gently winding streams such as natural rivers, the nonlinear terms and the terms divided by R which appear in the equation of motion (6) scarcely affect the distribution of the secondary flow. Therefore, the method proposed here can be applied to the natural meandering rivers as for as the conditions adopted in this paper are satisfied.

REFERENCES

1) Rozovskii, I. L.: Flow of Water in Bends of Open Channel, Academy Sciences of the USSR, 1957.

2) Yen, B. C.: Characteristics of Subcritical Flow in a Meandering Channel, Institute of Hydraulic Research, The University of Iowa, 1965.

3) Muramoto, Y.: Internal Structure of Flow through Curved Open Channel (II), Disaster Prevention Research Institute Annuals, No. 9, 1966. (in Japanese)

4) Kikkawa, H., S. Ikeda & Y. Kawamura: Secondary Flow in Curved Open Channels at the Fully Developed Region (I), Tech. Rep., No. 13, Dept. of Civil Eng., Tokyo Institute of Technology, 1972.

5) Kikkawa, H. & S. Ikeda: Flow through Curved Open Channels, Proc. 27th Annual Meeting, JSCE, II-87, 1972. (in Japanese)

6) Ippen, A. T. & P. A. Drinker: Boundary Shear Stress in Curved Trapezoidal Channels, Proc. ASCE, Vol. 88, No. HY 5, 1962.

7) Goncharov, V. N.: Dynamics of Channel Flow, Israel Program for Scientific Translations, 1964.

APPENDIX—NOTATION

B : width of a circular channel

Fr : Froude number

g : acceleration of gravity

H : depth of flow at the center of a channel

i : inclination of the free surface in the tangential direction

i_R : inclination of the free surface in the radial direction

K : parameter used in the quadratic pa-

rabola
K_s : roughness of the bottom
P : pressure
Q : total discharge
R, θ, Z : cylindrical coordinates
R_i, R_c, R_o : inner, central, and outer radius of a circular channel
Re : Renolds number
U, V, W : velocity components of the radial, tangential, and vertical directions in the cylindrical coordinates
V_0 : tangential velocity at the free surface at the center of a channel
V_a : average velocity ($=Q/A$)
V_* : shear velocity
x : distance from the outer wall in the radial direction (Fig. 1)
δ : thickness of the turbulent boundary layer at the bottom (the plane displaced above the bottom by δ is the virtual bottom)
ε : eddy viscosity ($=V_*H/15$)
ζ : distance from the inner wall in the radial direction (Fig. 1)
η : Z/H
Θ_c : central angle of bend
κ : Karman constant
ν : kinematic viscosity
ξ : vorticity of the secondary flow
τ_{R0} : boundary shear stress at the bottom
ψ : stream function of the secondary flow

(*Received May 15, 1973*)